A POLARIZABILITY MATRIX REPRESENTATION OF ELECTRICALLY SMALL OBSTACLES

A. O. Yee, et al

Ohio State University

Prepared for:

Air Force Office of Scientific Research

November 1973

UNCLASSIFIED
SECURITY CLASSIFICATION OF THIS PAGE (When Data Entered)

AD-773810

REPORT DOCUMENTATION PAGE	READ INSTRUCTIONS BEFORE COMPLETING FORM
AFOSR - TR - 74 - 0118	2. GOVT ACCESSION NO. / 3. RECIPIENT'S CATALOG NUMBER
4. TITLE (and Subtitle) A POLARIZABILITY MATRIX REPRESENTATION OF ELECTRICALLY SMALL OBSTACLES	5. TYPE OF REPORT & PERIOD COVERED Interim 6. PERFORMING ORG. REPORT NUMBER 2768-11
7. AUTHOR(s) A. O. Yee R. J. Garbacz	8. CONTRACT OR GRANT NUMBER(s) AFOSR 69-1710
9. PERFORMING ORGANIZATION NAME AND ADDRESS ElectroScience Laboratory Ohio State University Columbus, Ohio 43212	10. PROGRAM ELEMENT, PROJECT, TASK AREA & WORK UNIT NUMBERS 61102F 9769-02
11. CONTROLLING OFFICE NAME AND ADDRESS Air Force Office of Scientific Research/NM 1400 Wilson Blvd Arlington, VA 22209	12. REPORT DATE November 1973 13. NUMBER OF PAGES 21
14. MONITORING AGENCY NAME & ADDRESS(if different from Controlling Office)	15. SECURITY CLASS. (of this report) UNCLASSIFIED 15a. DECLASSIFICATION/DOWNGRADING SCHEDULE

16. DISTRIBUTION STATEMENT (of this Report)

Approved for public release; distribution unlimited.

17. DISTRIBUTION STATEMENT (of the abstract entered in Block 20, if different from Report)

18. SUPPLEMENTARY NOTES

19. KEY WORDS (Continue on reverse side if necessary and identify by block number)

polarizability, dipole, moments, discrimination, low frequency, scattering

20. ABSTRACT (Continue on reverse side if necessary and identify by block number)

A polarizability matrix representation is developed to describe the interaction of a plane electromagnetic wave with a loss-free body of arbitrary shape and small electrical size. This matrix is used to express far scattered fields in terms of six induced dipole moments - 3 mutually orthogonal dipoles of electric type and 3 mutually orthogonal dipoles of magnetic type. The matrix elements are evaluated from scattering data obtained by an independent method, such as the method of moments. Some numerical results for a variety

(continued)

DD FORM 1 JAN 73 1473 EDITION OF 1 NOV 65 IS OBSOLETE

UNCLASSIFIED
SECURITY CLASSIFICATION OF THIS PAGE (When Data Entered)

20. (continued)

of wire structures are presented in graphical form and compared with results obtained by numerical solutions to the corresponding boundary value problems.

A POLARIZABILITY MATRIX REPRESENTATION OF ELECTRICALLY SMALL OBSTACLES

A.O. Yee and R.J. Garbacz

TECHNICAL REPORT 2768-11

November 1973

Grant AFOSR 69-1710A

Department of the Air Force
Air Force Office of Scientific Research
Arlington, Virginia 22209

TABLE OF CONTENTS

I. INTRODUCTORY REMARKS

A difficult and vexing problem in electromagnetic theory is the discrimination of obstacle shapes by far-field scattering measurements. The voluminous data usually taken, the ordering and reduction of these data, the compromises which must be made in choice of measurement parameters, such as frequency, polarization, etc., all compound the problem and make it quite difficult to extract the shape-dependent essence upon which to base a discrimination scheme.

Although this report hardly solves the problem it does present a view point which may be useful. This viewpoint recognizes that a good deal of information about an obstacle is contained in low frequencies[1,2,3], i.e., those where the obstacle is only a fraction of a wavelength in maximum dimension. At such low frequencies, it is assumed that an exciting plane wave induces in the obstacle only six modes causing scatter - three electric dipoles oriented along the three orthogonal axes of a Cartesian coordinate system chosen within the body, and three magnetic dipoles oriented along those same axes. The relative strengths of these six induced dipoles are proportional to the incident electric or magnetic fields colinear with them and the proportionality constants may be arranged to form a polarizability matrix. The terminology, "polarizability matrix", is familiar in the theory of electrostatic and magnetic static fields[4,5] and has been applied to quasistatic fields as well[6,7]. We have carried it over to the regime of quasistatic fields by relaxing two constraints. First, and in contrast with the static case where the polarizability matrix has all real elements, we allow the elements of our matrix to become complex, thereby permitting depolarization effects other than linear-to-linear. Second, and again in contrast with the static case where electric and magnetic dipoles are all uncoupled, we allow such coupling to manifest itself in non-zero off-diagonal matrix elements.

The 36 elements of the 6x6 polarizability matrix are determined by illuminating the obstacle in turn with six different excitations - each one designed to most strongly induce only one of the dipoles mentioned above. The far-scattered field resulting from each such excitation is then calculated by computerized boundary solution technique, such as reaction matching introduced by Richmond[8]. The reactions of each of the six dipole fields with each of the six scattered fields (36 reactions in all) are then evaluated over the sphere at infinity, thereby determining the 36 elements of the polarizability matrix. (Actually, matrix symmetry reduces the maximum number of necessary reactions to 21.)

Assuming the validity of the model, knowledge of the polarizability matrix permits the evaluation of the far-field scattered in any direction due to a plane wave of any polarization incident from any direction, all at a chosen frequency. Such generality gives us some confidence that the polarizability matrix of a given obstacle is an almost unique

mathematical representation of that obstacle ("almost", because absolute uniqueness requires knowledge of the polarizability matrix over a range of frequencies - this has not been investigated). If such a one-to-one correspondence between an obstacle shape and a matrix can be assumed, we have here a mathematical model which is suited to processing by computer for shape discrimination purposes. For example, if $[\alpha_1]$ and $[\alpha_2]$ are polarizability matrices representing two obstacles, a decision-making process could be based on the complex parameter,

$$D \equiv \frac{[\alpha_1][\alpha_2]^{ct}}{\sqrt{||\alpha_1|| \cdot ||\alpha_2||}} ,$$

where $[\ ]^{ct}$ means "complex conjugate transpose of" and $||\ ||$ means "norm of". Or, perhaps the elements of $[\alpha_1]$ and $[\alpha_2]$ can locate two points in a complex 21-dimensional space, the distance between them, defined by a suitably chosen norm, serving as the basis of a decision-making process.

The last suggestion brings to fore a basic weakness of the polarizability matrix description of an obstacle, and that is its dependence on the location and orientation of the coordinate system chosen within it. Thus, an obstacle is represented not by a unique matrix, but by a set of matrices (ideally) related to each other by rotation and translation operations. The best one can hope for is to choose coordinates which cause the six dipoles to be characteristic modes[9,10,11,12] of the obstacle, that is, which cause the six dipoles to be located and oriented in such a manner that each one is excited to a strength proportional to its own normalized radiation pattern. If this can be achieved, then only six complex numbers (which are unique to within the accuracy of the dipole approximation in the form of a diagonal matrix) suffice to describe the obstacle and can therefore be used as a basis for discrimination. The relationship between the polarizability matrix and the characteristic matrix representations has not been developed so far.

In this report we present a set of sample data in graphical form comparing the backscattering cross sections of a variety of perfectly conducting wire obstacles as obtained by reaction matching and approximated by the polarizability matrix formulation. The theoretical development of this formulation is given in the Appendix.

II. NUMERICAL RESULTS

Numerical results, comparing backscattering patterns calculated using Richmond's reaction matching technique and the polarizability matrix, were calculated for several simple configurations - the linear wire, the linear wire tilted, the square loop, a cube and a rectangular box, both outlined by wires.

Figures 1-3 show backscattering cross sections of three lengths of

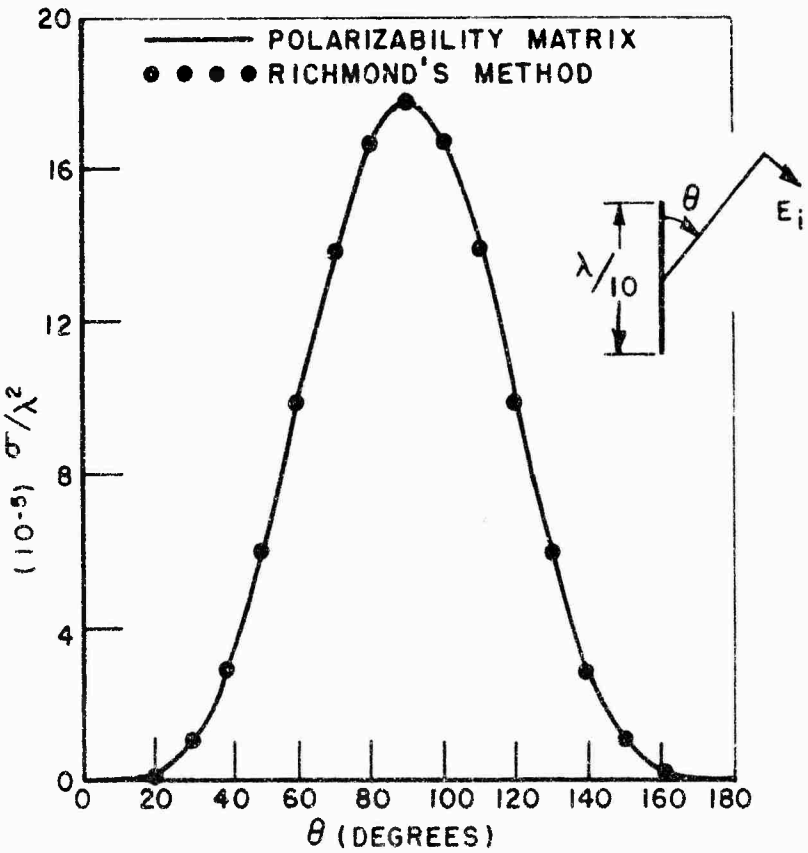

Fig. 1. Backscattering cross section as a function of incident angle θ for a dipole of length = 0.1λ and radius = 0.005λ. The incident electric field is θ-polarized.

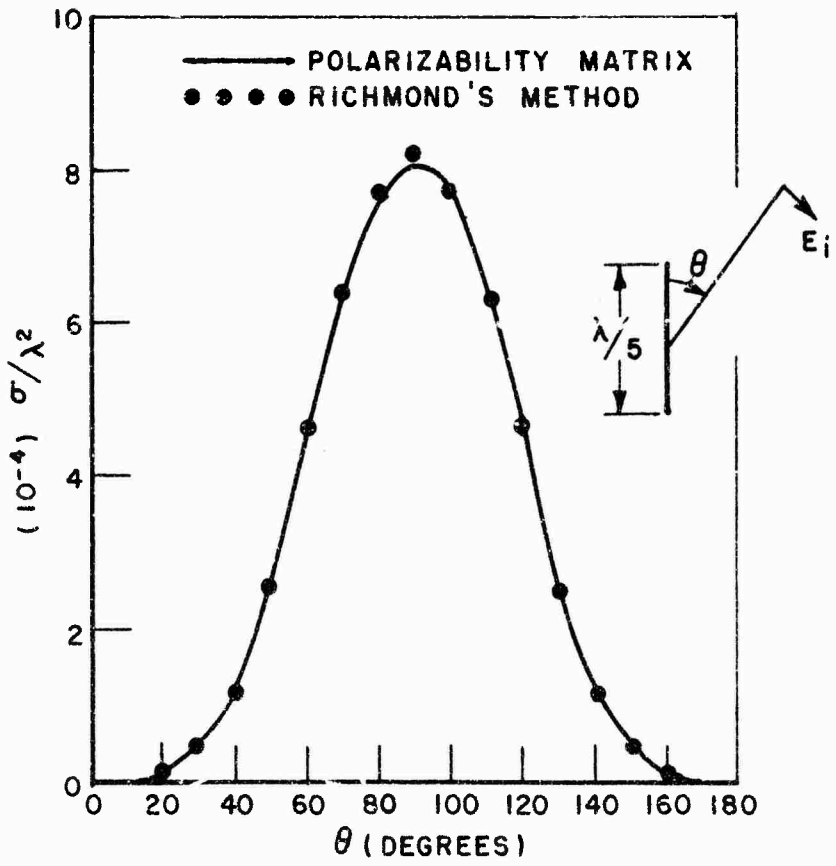

Fig. 2. Backscattering cross section as a function of incident angle θ for a dipole of length = 0.2λ and radius = 0.005λ. The incident electric field is θ-polarized.

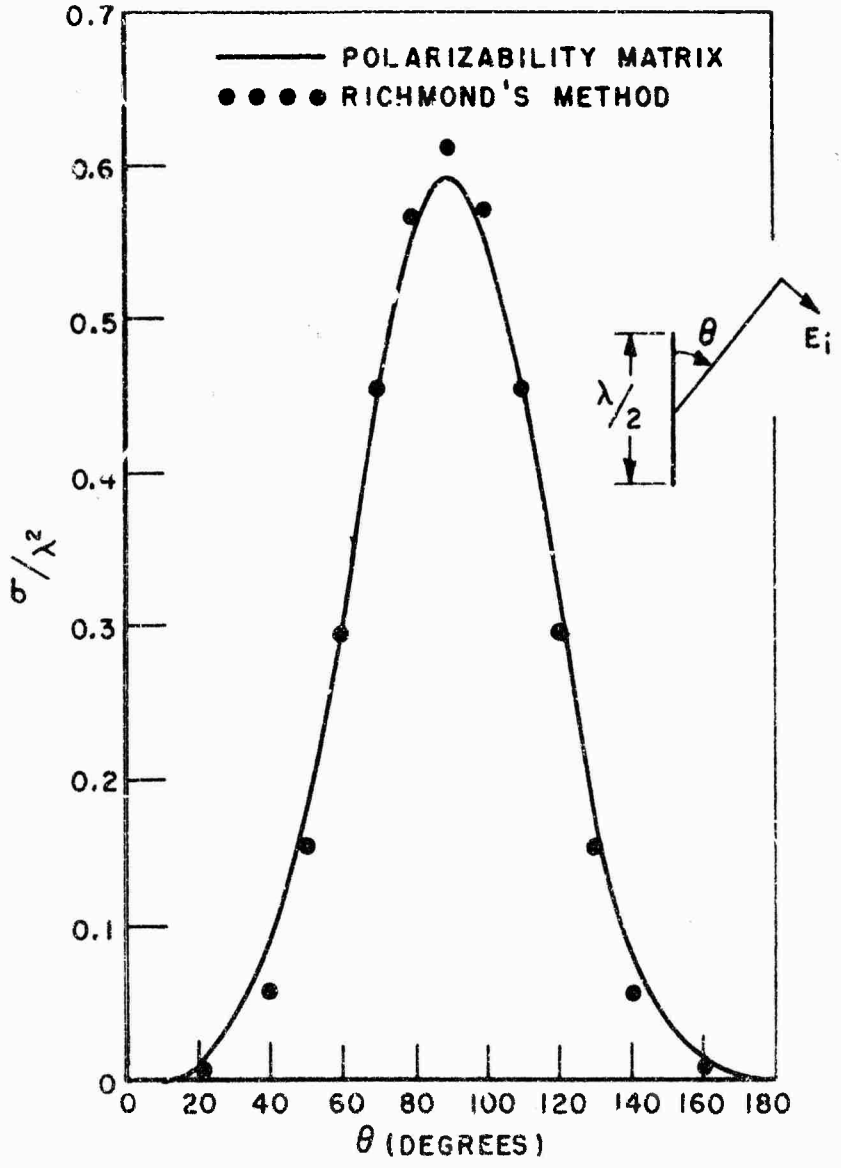

Fig. 3. Backscattering cross section as a function of incident angle θ for a dipole of length = 0.5λ and radius = 0.055λ. The incident electric field is θ-polarized.

linear wire, λ/10, λ/5, λ/2, with relative orientations of wire and electric field polarization indicated. Figures 4-5 show backscatter

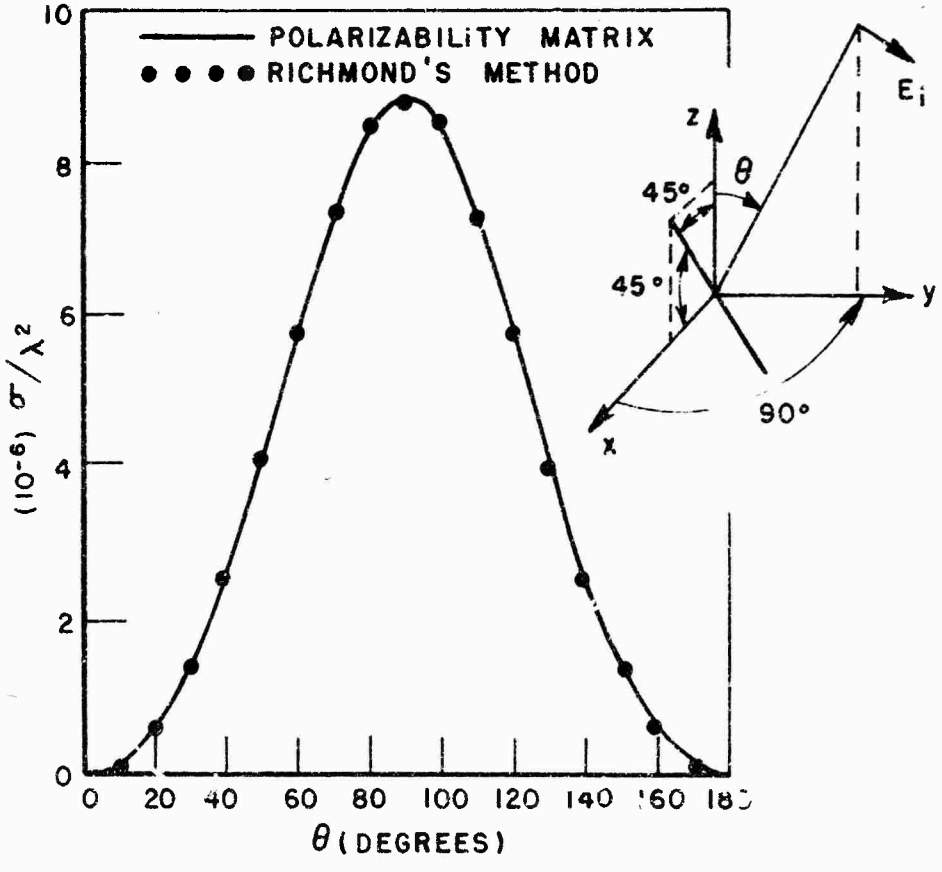

Fig. 4. Backscattering cross section as a function of incident angle θ for a tilted dipole of length = 0.1λ and radius = 0.005λ. The incident electric field is θ-polarized.

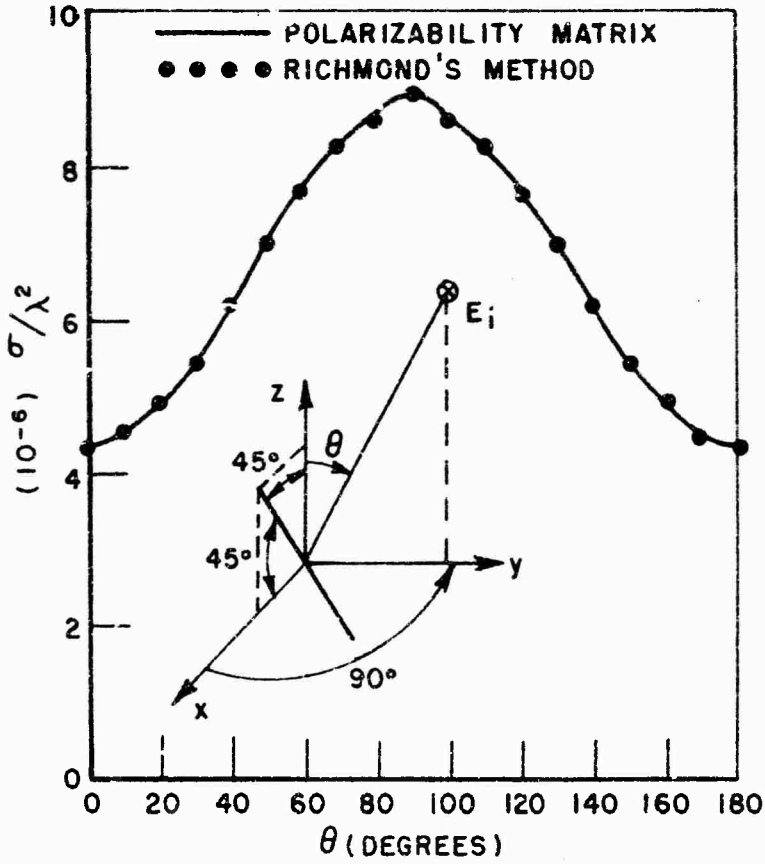

Fig. 5. Backscattering cross-section as a function of incident angle θ for a tilted dipole of length = 0.1λ and radius = 0.005λ. The incident electric field is ϕ-polarized.

data for a tilted wire of length λ/10 illuminated in two polarizations. Similar data for a wire of length λ/5 are shown in Figs. 6-7.

Figures 8-9 show backscattering patterns of a square loop, λ/10 on a side in two polarizations, and Figs. 10 and 11 show similar data for a cube λ/25 on a side and a rectangular box λ/25 x λ/25 x λ/15 in dimension. Both of these latter obstacles are not solid bodies but wire outlines as indicated in the figures.

All cases presented show good agreement with the "exact" solution of Richmond. Although not plotted, phase patterns are equally good. However, for obstacles larger than the ones shown, the polarizability matrix representation quickly loses accuracy, particularly for the more complex shapes. The limitation to cubes, for example, about λ/25 on a side is disappointingly restrictive and severely limits the practical use of the representation.

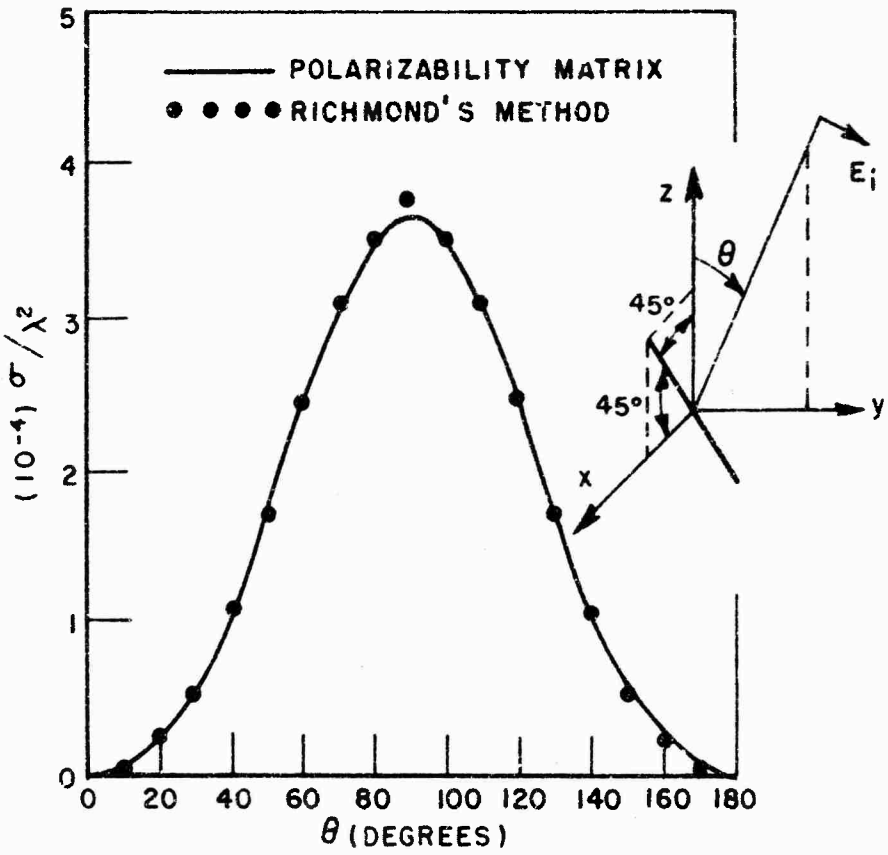

Fig. 6. Backscattering cross section as a function of incident angle θ for a tilted dipole of length = 0.2λ and radius = 0.005λ. The incident electric field is θ-polarized.

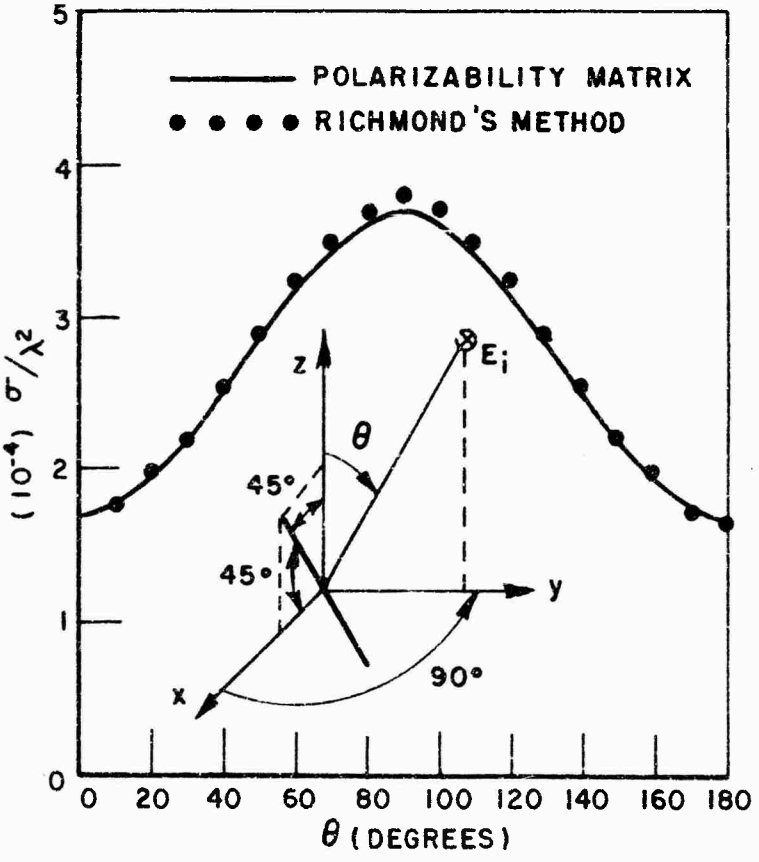

Fig. 7. Backscattering cross section as a function of incident angle θ for a tilted dipole of length = 0.2λ and radius = 0.005λ. The incident electric field is ϕ-polarized.

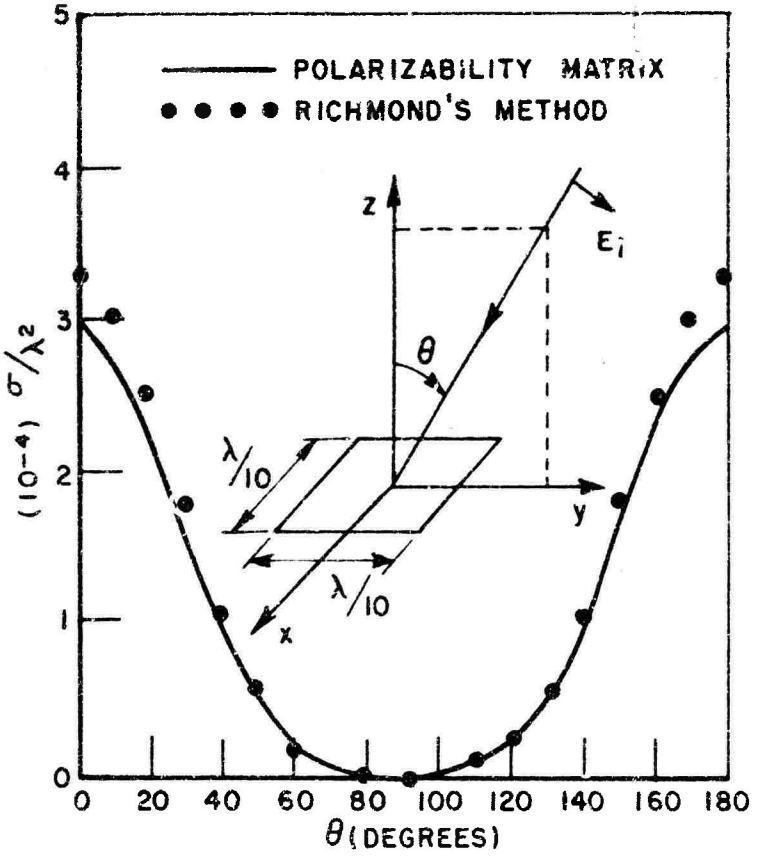

Fig. 8. Backscattering cross section as a function of incident angle θ for a square loop of edge = 0.1λ and wire radius = 0.005λ. The incident electric field is θ-polarized.

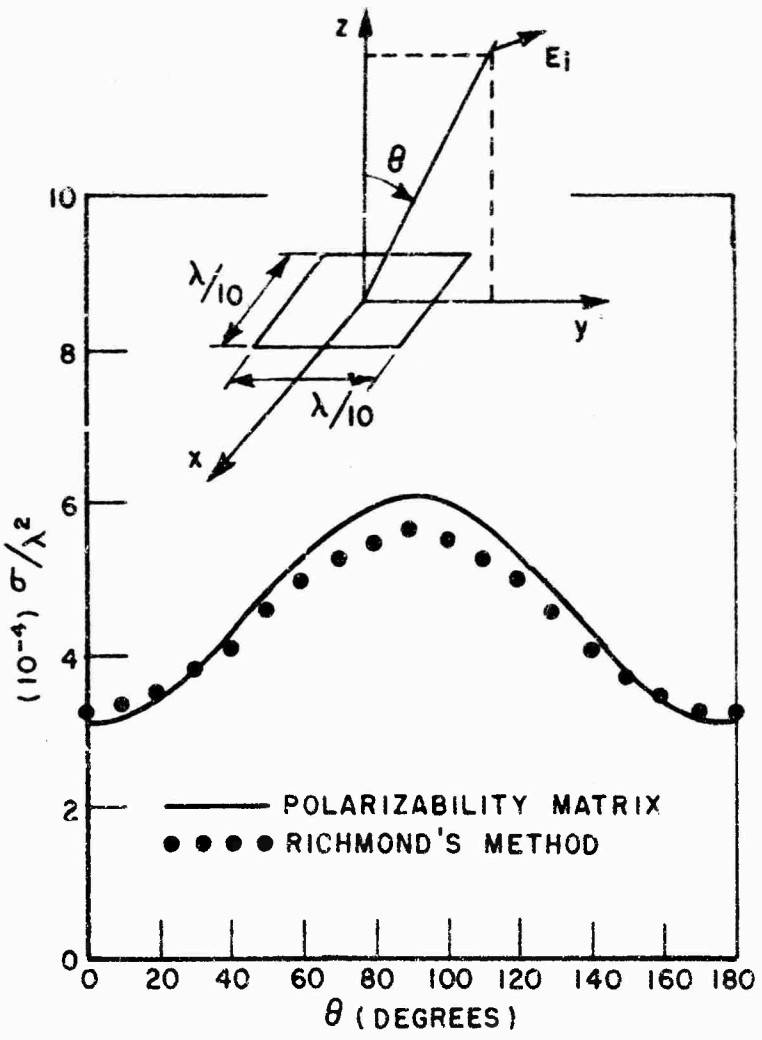

Fig. 9. Backscattering cross section as a function of incident angle θ for a square loop of edge = 0.1λ and wire radius = 0.005λ. The incident electric field is ϕ-polarized.

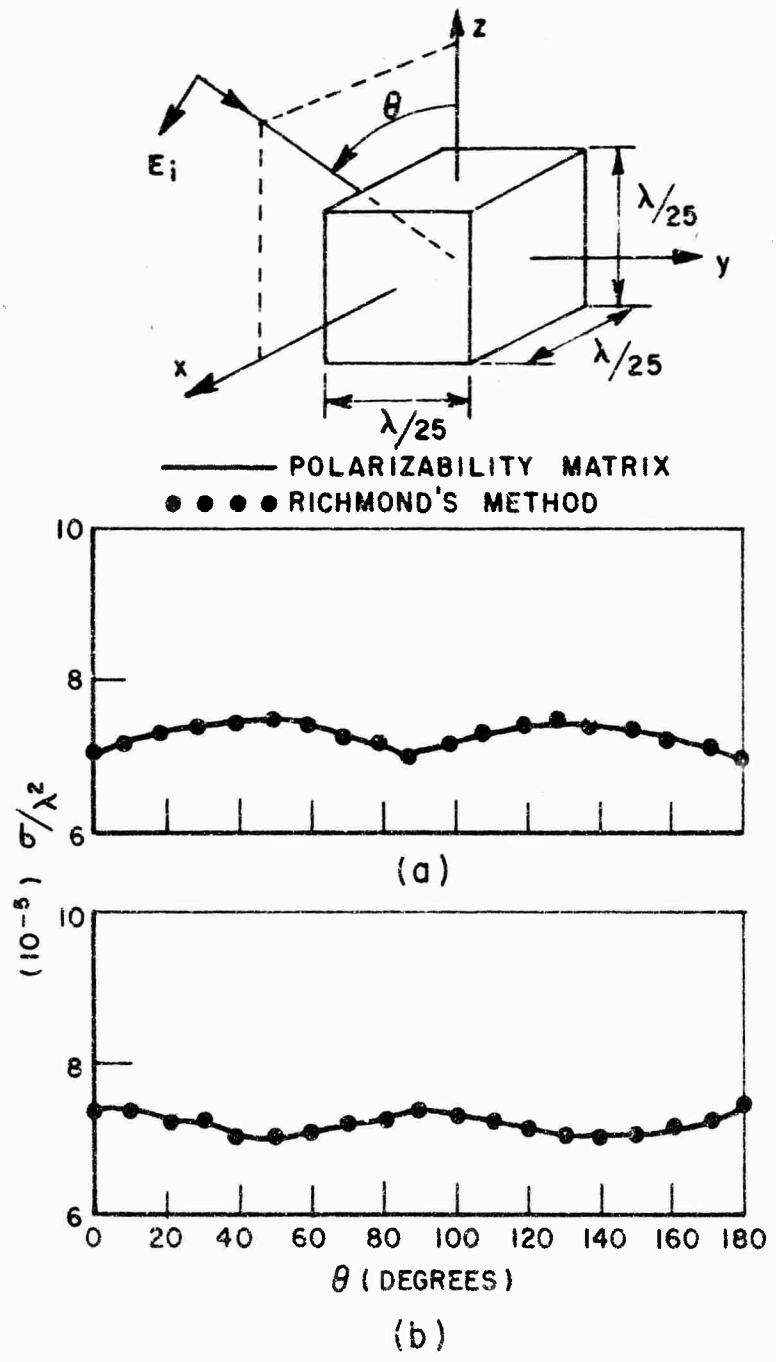

Fig. 10. Backscattering cross section as a function of incident angle θ for a cube of edge = 0.04λ.
(a) The incident electric field is θ-polarized.
(b) The incident electric field is ϕ-polarized.

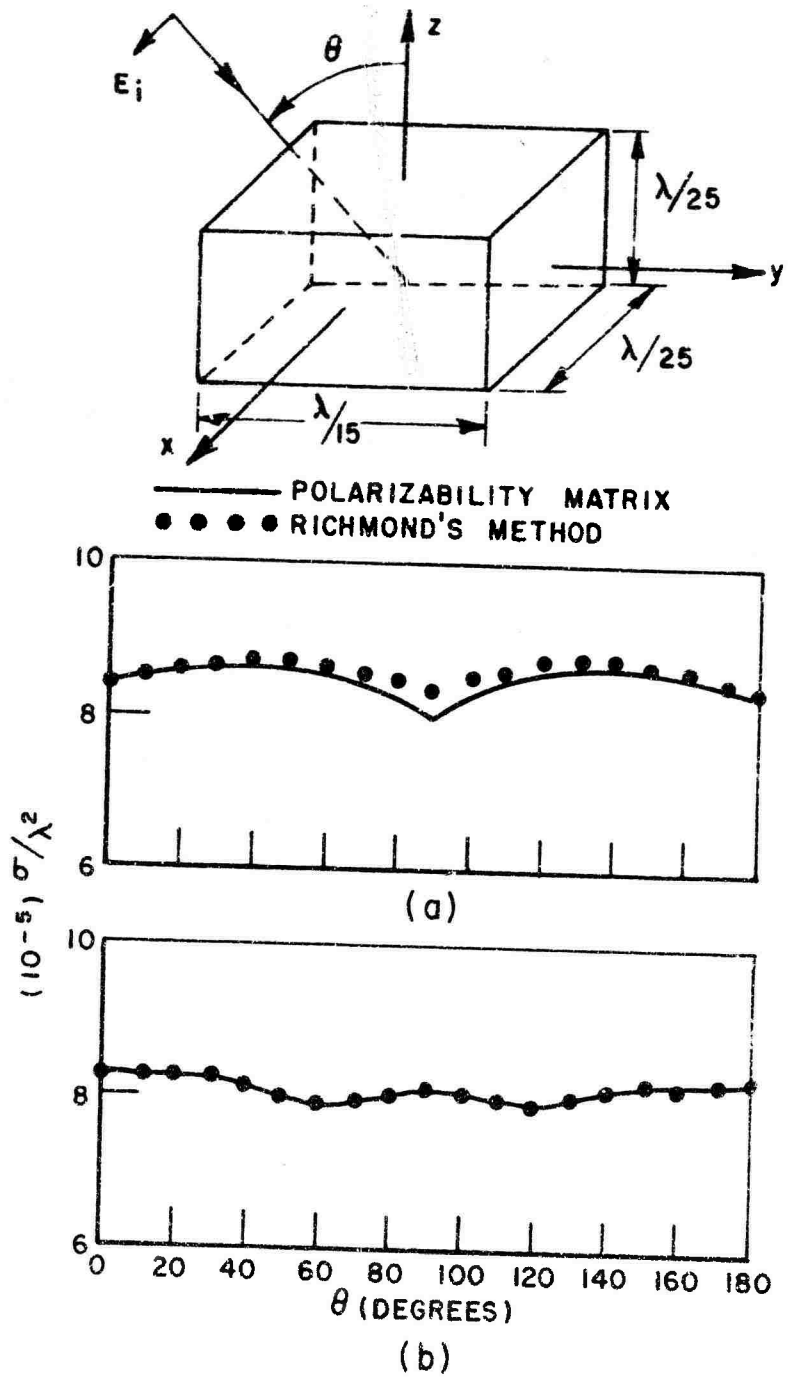

Fig. 11. Backscattering cross section as a function of incident angle for a rectangular box.
(a) The incident electric field is θ-polarized.
(b) The incident electric field is φ-polarized.

III. CONCLUSIONS

For electrically small obstacles (by which we mean obstacles at most a fraction of a wavelength, i.e., $\lambda/5$ - $\lambda/25$ in maximum dimension) the polarizability matrix representation is an accurate description of the scattering properties of obstacles. This size limitation is smaller than envisioned for obstacles pertinent to the objectives of the present grant. The addition of multipoles of higher order than the dipole would improve the representation and probably would extend its accuracy to larger bodies, but at severe expense of simplicity. Additionally, there remains the question of how discriminatory is the polarizability matrix representation, that is, how "different" are the matrices associated with obstacles of differing shapes, so that they can be used as sensitive and reliable discriminators of shape. Further investigation into such questions is of interest, but cannot be recommended at the present time in view of the aims of the present grant.

REFERENCES

1. Kennaugh, E.M. and Moffatt, D.L., "Transient and Impulse Response Approximations," Proc. IEEE, Vol. 53, No. 8, August 1965, pp. 893-901.

2. Moffatt, D.L. and Young, J.D., "Measured Radar Spectral Signatures," Proc. of the 1970 Tri-Service Radar Symposium, Colorado Springs, Colorado.

3. Hill, D.A., "Electromagnetic Scattering Concepts Applied to the Detection of Targets Near the Ground," Ph.D. Dissertation, The Ohio State University, 1970.

4. Van de Hulst, H.C., Light Scattering by Small Particles, John Wiley and Sons, Inc., New York, 1957, pp. 302-304.

5. Landau, L.D. and Lifshitz, E.M., E.M., Electrodynamics of Continuous Media, Pergamon Press, 1960, pp. 7 and 192.

6. Keller, J.B., Kleinman, R.E. and Senior, T.B.A., "Dipole Moments in Rayleigh Scattering," J. Inst. Maths. Applics, No. 9, 1972, pp. 14-22.

7. Kleinman, R.E. and Senior, T.B.A., "Rayleigh Scattering Cross Sections," Radio Science, Vol. 7, No. 10, October 1972, pp. 937-942.

8. Richmond, J.H., "Computer Program for Thin-Wire Structures in a Homogeneous Conducting Medium," Report 2902-12, August 1973, ElectroScience Laboratory, Department of Electrical Engineering, The Ohio State University Research Foundation; prepared under Grant No. NGL 36-008-138 for National Aeronautics and Space Administration.

9. Garbacz, R.J., "Modal Expansions for Resonance Scattering Phenomena," Proc. IEEE, Vol. 53, No. 8. August 1965, pp. 856-864.

10. Garbacz, R.J., "A General Expansion for Radiated and Scattered Fields," IEEE Trans. on Ant. and Prop., Vol. AP-19, No. 3, May 1971, pp. 348-358.

11. Harrington, R.F. and Mautz, R., "Theory of Characteristic-Modes for Conducting Bodies," IEEE Trans. on Ant. and Prop., Vol. AP-19, No. 5, September 1971, pp. 622-628.

12. Harrington, R.F. and Mautz, R., "Computation of Characteristic-Modes for Conducting Bodies," IEEE Trans. on Ant. and Prop., Vol. AP-19, No. 5, September 1971, pp. 629-639.

APPENDIX I
THEORETICAL DEVELOPMENT

At very low frequencies, the fields scattered by an obstacle arise from two induced dipole moments, one electric and one magnetic, each of which may be decomposed into three dipoles along three mutually perpendicular axes of a Cartesian coordinate system (Fig. I-1) chosen

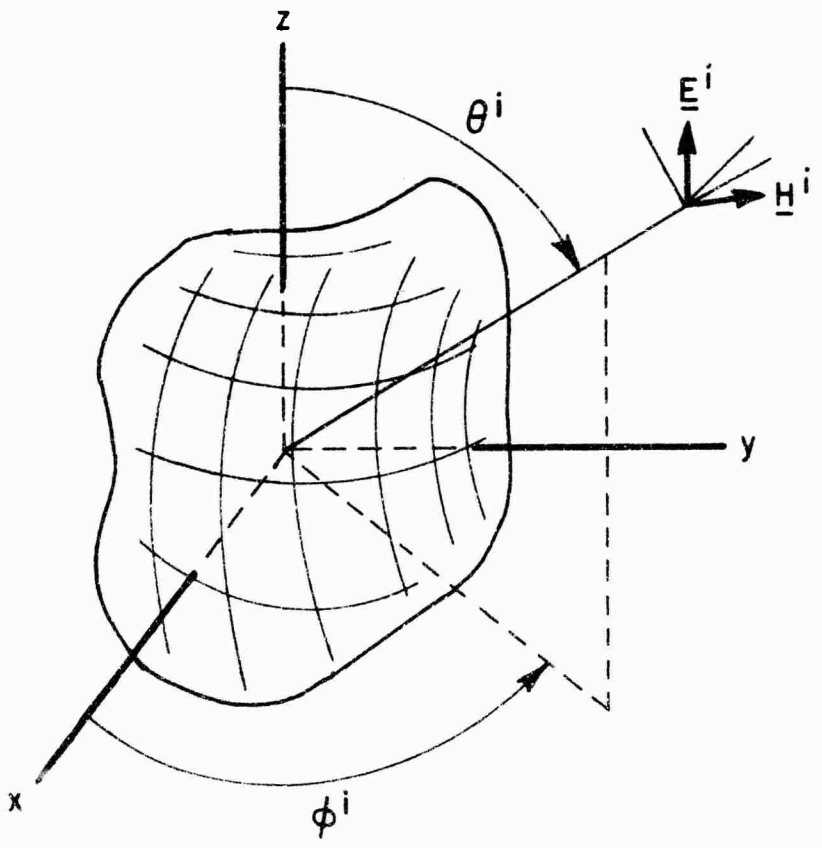

Fig. I-1. Polar coordinate system.

within the obstacle. The six induced dipole moments, p_{ex}, p_{ey}, p_{ez}, p_{mx}, p_{my}, p_{mz}, (Fig. I-2) are complex and are related to the exciting electric and magnetic fields ($\underline{E}^i$,$\underline{H}^i$) by

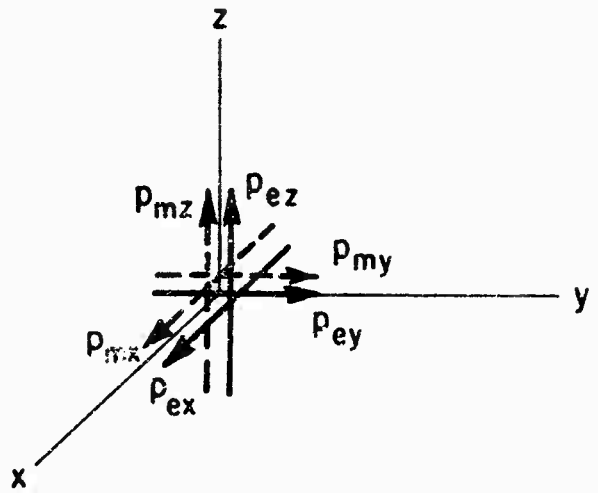

Fig. I-2. Sketch of six dipole moments induced in an obstacle.

$$(1)\qquad \begin{pmatrix} p_{ex} \\ p_{ey} \\ p_{ez} \\ \hline p_{mx} \\ p_{my} \\ p_{mz} \end{pmatrix} = \left[\begin{array}{ccc:ccc} \alpha_{ex}^{ex} & \alpha_{ey}^{ex} & \alpha_{ez}^{ex} & \alpha_{mx}^{ex} & \alpha_{my}^{ex} & \alpha_{mz}^{ex} \\ \alpha_{ex}^{ey} & \alpha_{ey}^{ey} & \alpha_{ez}^{ey} & \alpha_{mx}^{ey} & \alpha_{my}^{ey} & \alpha_{mz}^{ey} \\ \alpha_{ex}^{ez} & \alpha_{ey}^{ez} & \alpha_{ez}^{ez} & \alpha_{mx}^{ez} & \alpha_{my}^{ez} & \alpha_{mz}^{ez} \\ \hdashline \alpha_{ex}^{mx} & \alpha_{ey}^{mx} & \alpha_{ez}^{mx} & \alpha_{mx}^{mx} & \alpha_{my}^{mx} & \alpha_{mz}^{mx} \\ \alpha_{ex}^{my} & \alpha_{ey}^{my} & \alpha_{ez}^{my} & \alpha_{mx}^{my} & \alpha_{my}^{my} & \alpha_{mz}^{my} \\ \alpha_{ex}^{mz} & \alpha_{ey}^{mz} & \alpha_{ez}^{mz} & \alpha_{mx}^{mz} & \alpha_{my}^{mz} & \alpha_{mz}^{mz} \end{array}\right] \begin{pmatrix} E_x^i \\ E_y^i \\ E_z^i \\ \hline H_x^i \\ H_y^i \\ H_z^i \end{pmatrix}$$

or

$$(2)\qquad (p) = [\alpha](F^i)$$

where $(F^i) = \begin{pmatrix} E^i_x \\ E^i_y \\ E^i_z \\ H^i_x \\ H^i_y \\ H^i_z \end{pmatrix}$ is a column vector composed of the Cartesian components of the exciting electric and magnetic fields at the chosen origin. They may be complex.

$[\alpha]$ is defined to be the polarizability matrix.

If the electric and magnetic fields are those of a plane wave, then the vector (F^i) is understood to depend upon the polarization state and direction of incidence of the plane wave with respect to the chosen coordinate system. The components of the polarizability matrix depend only upon the obstacle shape and composition and the coordinate choice.

In matrix notation, the far electric field pattern evaluated in the (θ^s,ϕ^s) direction may be obtained from

(3)

$$\begin{pmatrix} E^s_\theta \\ E^s_\phi \end{pmatrix} = \sqrt{\frac{3Z_o}{8\pi}} \begin{bmatrix} -\cos\theta^s\cos\phi^s & -\cos\theta^s\sin\phi^s & \sin\theta^s & \sin\phi^s & -\cos\phi^s & 0 \\ \sin\phi^s & -\cos\phi^s & 0 & \cos\theta^s\cos\phi^s & \cos\theta^s\sin\phi^s & -\sin\theta^s \end{bmatrix} \begin{pmatrix} p_{ex} \\ p_{ey} \\ p_{ez} \\ p_{mx} \\ p_{my} \\ p_{mz} \end{pmatrix},$$

or

(4) $(E^s) = [R]\,(p)$,

where $Z_0 = 120\pi$ and the constant $\frac{3Z_0}{8\pi}$ normalizes the R matrix such that a unit induced dipole moment, e.g., p_{ex}, radiates unit power. Combining Eqs. (2) and (4), we obtain an expression for the far field scattering pattern due to a plane wave arriving from any direction,

$$(E^s) = [R]\,[\alpha]\,(F^i). \tag{5}$$

To determine the elements of the polarizability matrix, we illuminate the obstacle with 6 different excitations, each of which causes the (F^i) matrix to exhibit only one non-zero component. Each such excitation consists of two plane waves traveling in opposite directions along the 3 principal coordinate directions, and polarized constructively or destructively to produce a null in either the electric field or the magnetic field at the origin. The six excitations are pictured in Fig. I-3. The far electric field patterns scattered by each excitation can be calculated by an independent method such as Richmond's reaction matching[8] and are symbolized by $\underline{E}_{ex}$, $\underline{E}_{ey}$, $\underline{E}_{ez}$, $\underline{E}_{mx}$, $\underline{E}_{my}$, $\underline{E}_{mz}$, where the subscripts denote the type and direction of the field produced at the origin by the exciting wave.

If the far field patterns radiated by unit dipole moments are denoted by

$$\begin{aligned}
\underline{E}^{ex} &= \sqrt{\frac{3Z_0}{8\pi}}\,[-\hat{\theta}\cos\theta\cos\phi+\hat{\phi}\sin\phi],\\
\underline{E}^{ey} &= \sqrt{\frac{3Z_0}{8\pi}}\,[-\hat{\theta}\cos\theta\sin\phi-\hat{\phi}\cos\phi],\\
\underline{E}^{ez} &= \sqrt{\frac{3Z_0}{8\pi}}\,[\hat{\theta}\sin\theta],\\
\underline{E}^{mx} &= \sqrt{\frac{3Z_0}{8\pi}}\,[\hat{\theta}\sin\phi+\hat{\phi}\cos\theta\cos\phi],\\
\underline{E}^{my} &= \sqrt{\frac{3Z_0}{8\pi}}\,[-\hat{\theta}\cos\phi+\hat{\phi}\cos\theta\sin\phi],\\
\underline{E}^{mz} &= \sqrt{\frac{3Z_0}{8\pi}}\,[-\hat{\phi}\sin\theta],
\end{aligned} \tag{6}$$

where the superscripts denote the type and direction of the respective dipoles, then the elements of the polarizability matrix are given by the reactions,

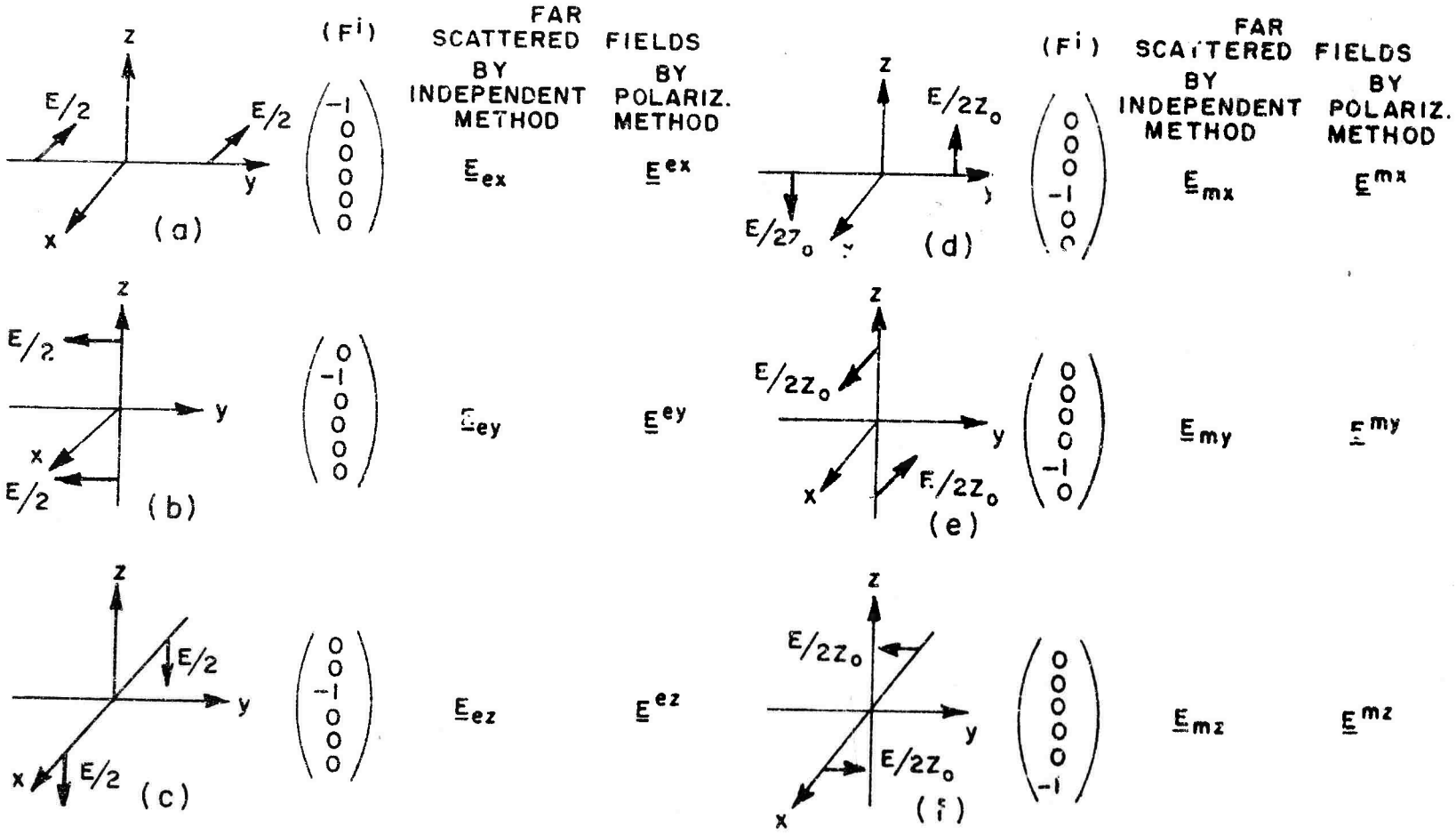

Fig. I-3. Six excitation configurations, their vector representations, and the far scattered fields associated with each (subscripts refer to fields calculated by an independent method, superscripts refer to fields calculated using the polarizability formulation).

$$\alpha_{ex}^{ex} = \frac{1}{Z_o} \oiint_{\Sigma} \underline{E}_{ex} \cdot \underline{E}^{ex} \sin\theta d\theta d\phi,$$

$$\alpha_{ex}^{ey} = \frac{1}{Z_o} \oiint_{\Sigma} \underline{E}_{ex} \cdot \underline{E}^{ey} \sin\theta d\theta d\phi, \tag{7}$$

$$\alpha_{ex}^{ez} = \frac{1}{Z_o} \oiint_{\Sigma} \underline{E}_{ex} \cdot \underline{E}^{ez} \sin\theta d\theta d\phi,$$

etc.

In these equations, $\underline{E}_{ex}$, etc., are known functions of (θ,ϕ) on the sphere Σ at infinity (from reaction matching) and $\underline{E}^{ex}$, etc., are known functions of (θ,ϕ) as well (from Eq. (6)), so it is only a matter of numerically integrating their dot product over Σ to find the elements of the polarizability matrix. In general 21 such reaction integrals must be evaluated.

Typical non-zero values of the polarizability matrix elements are, for the examples cited in the text of this report,

Fig. 1: $\alpha_{ez}^{ez} = 1.771\times10^{-4} - j8.796\times10^{-7}$

Fig. 2: $\alpha_{ez}^{ez} = 1.157\times10^{-3} - j3.735\times10^{-5}$

Fig. 3: $\alpha_{ez}^{ez} = -1.615\times10^{-2} - j2.788\times10^{-2}$

Fig. 4: Fig. 5: $\alpha_{ex}^{ex} = \alpha_{ex}^{ez} = \alpha_{ez}^{ex} = \alpha_{ez}^{ez} = 8.809\times10^{-5} - j4.374\times10^{-7}$

Fig. 6: Fig. 7: $\alpha_{ex}^{ex} = \alpha_{ex}^{ez} = \alpha_{ez}^{ex} = \alpha_{ez}^{ez} = 5.666\times10^{-4} - j1.829\times10^{-5}$

Fig. 8: Fig. 9: $\alpha_{ex}^{ex} = \alpha_{ey}^{ey} = 7.056\times10^{-4} - j1.434\times10^{-5}$

$$\alpha_{mz}^{mz} = -3.077\times10^{-4} - j2.666\times10^{-6}$$